Atmospheric Research 99 (2011) 353–364

Contents lists available at ScienceDirect

Atmospheric Research

journal homepage: www.elsevier.com/locate/atmos

Size-resolved hygroscopicity of submicrometer urban aerosols in Shanghai during wintertime

Xingnan Ye *, Zhen Ma, Dawei Hu, Xin Yang, Jianmin Chen *

Department of Environmental Science & Engineering, Fudan University, Shanghai 200433, China

ARTICLE INFO

Article history:
Received 18 August 2010
Received in revised form 3 November 2010
Accepted 7 November 2010

Keywords:
Hygroscopic behavior
Growth factor
Ambient aerosols
Yangtze River Delta

ABSTRACT

Information about the hygroscopic growth factors and mixing state is important for understanding the haze formation mechanism in the highly polluted Yangtze River Delta. Herein, the size-resolved hygroscopicity of ambient aerosols in Shanghai was studied during wintertime. The hygroscopic growth factors were measured using a Hygroscopic Tandem Differential Mobility Analyzer (HTDMA) for dry particles with diameters of 30–250 nm on the campus of Fudan University. A modal external mixture containing two hygroscopic groups was observed. The mean hygroscopic growth factors of the less-hygroscopic group at 85% relative humidity were lower than 1.10, and the average number fraction of the less-hygroscopic group varied in the range of 0.33–0.17, decreasing slightly with the increase of dry particle size. The mean hygroscopic growth factors of the more-hygroscopic group showed there was a significant difference between Aitken and accumulation mode particles, nearly 1.3 for Aitken mode particles and above 1.4 for accumulation mode particles. On the basis of the ammonium sulfate model, the average hygroscopic volume fraction of the more-hygroscopic particles was estimated to be in the range of 0.47–0.70, and there was a large gap between the hygroscopic volume fractions of Aitken and accumulation mode particles. The hygroscopic growth against relative humidity test not only showed that deliquescence relative humidity depended on particle size, but also revealed that the addition of nitrate on the particles was initially promoted by sulfate condensation. The results also suggested that most accumulation mode particles were deliquesced under haze conditions.

1. Introduction

With its rapid industrial development and urbanization in the past 20 years, air pollution in China's megacities has drawn increasing attention. Primary emissions due to fossil fuel consumption, together with secondary aerosols formed by photochemical oxidation and heterogeneous reactions, pose great threats to the health and environment of urban residents. Haze, a phenomenon characterized by low visibility (<10 km), is caused by high concentration of particulate pollutants. The Yangtze River Delta (YRD) is one of the four heaviest haze regions in China. As the economic center of the YRD, Shanghai contributed 4.6% of the national GDP in 2008. As the largest megacity in China, there are more than 18 million residents and 2.38 million automobiles in Shanghai (Geng et al., 2008). It was concluded, based on previous observation, that the visibility decrease during haze episode was largely dependent on the increase of PM2.5 concentration (Fu et al., 2008).

Atmospheric visibility is influenced by many factors such as chemical composition, particle size distribution, aerosol formation, and the aerosol mixing state. The presence of an aqueous phase facilitates heterogeneous reactions of nitric acid with sea salt and mineral dust (Liu et al., 2007, 2008), N_2O_5 hydrolysis on tropospheric aerosol surface (Dentener and Crutzen, 1993; Mogili et al., 2006), and sulfate formation

* Corresponding authors. Tel.: +86 21 65642526; fax: +86 21 65642080.
E-mail addresses: yexingnan@fudan.edu.cn (X. Ye), jmchen@fudan.edu.cn (J. Chen).

0169-8095/$ – see front matter © 2010 Elsevier B.V. All rights reserved.
doi:10.1016/j.atmosres.2010.11.008

under haze conditions (Tursic et al., 2004). The hygroscopic growth of ambient aerosols may change both the particle size and optical properties (Gasso e al., 2000; Kotchenruther et al., 1999; Swietlicki et al., 1999). The light scattering property as a function of relative humidity (RH) is one parameter to estimate the direct effect of aerosols on climate, and some attempts have been made to incorporate the hygroscopic growth factor into global climate models (Boucher and Anderson, 1995; Randall et al., 2007). The hygroscopic behavior of atmospheric aerosol may affect its ability to serve as cloud condensation nuclei (Petters and Kreidenweis, 2007; Svenningsson et al., 2006), which is the key parameter for determining the indirect climate effect of aerosols. In a recent work, Zhang et al. (2008) reported that the condensation of sulfuric acid followed by hygroscopic growth could enhance the optical properties of soot aerosols remarkably. In addition, the health effects of aerosol particles partly depend on the deposition site in the respiratory tract that is directly affected by hygroscopic properties (Chan et al., 2002; Londahl et al., 2007).

Many techniques such as nephelometry (Day et al., 2006; Liu et al., 2008; Rood et al., 1985), electrodynamic balance (Davis et al., 1990; Peng and Chan, 2001), and tandem differential mobility analyzer (TDMA) (Liu et al., 1978) have been employed to measure the hygroscopic behavior of ambient aerosols. As the only in-situ instrument that is able to determine water uptake as well as to probe the mixing state in terms of hygroscopicity, hygroscopic TDMA (HTDMA) has become the most commonly employed instrument for observing the hygroscopic behavior of ambient aerosols (Swietlicki et al., 2008). Since the pioneering work of McMurry and Stolzenburg (1989), the hygroscopic growth of urban aerosol particles has attracted much interest (Aggarwal et al., 2007; Baltensperger et al., 2002; Chen et al., 2003; Cocker et al., 2001; Ferron et al., 2005; Massling et al., 2005). Notably, field observations on the aerosol hygroscopic properties were recently deployed in Beijing, North China Plain, and the Pear River Delta (Achtert et al., 2009; Eichler et al., 2008; Massling et al., 2009; Yan et al., 2009).

There have been limited studies on haze pollution in the YRD (Fu et al., 2008; Wang et al., 2006; Xiu et al., 2004), and no information on aerosol hygroscopicity has been reported in these studies. Herein, we present field measurements of the size-resolved hygroscopicity of urban ambient aerosols in Shanghai. Through TDMA inversion and chemical composition modeling, the characteristics of the aerosol mixing state are discussed.

2. Experimental

2.1. HTDMA system

A detailed description of the custom-built HTDMA was published elsewhere (Ye et al., 2009). Fig. 1 presents a schematic diagram of the HTDMA. The system can be operated as a scanning mobility particle sizer (SMPS) and a TDMA, alternatively. To maintain a gas phase composition in the sheath air similar to the sample, sheath and excess flows were coupled in a closed loop for DMA1 (Model 3081 L, TSI Inc.). Both sample and sheath gas RH were measured through HUMICAP180® capacitive sensor (HMM22D module, Vaisala Inc.) mounted before and after DMA2 to ensure a close RH value (within 2%) between the sheath flow and the sample flow. Prior to classification in DMA1, the aerosol sample was initially dried at RH<10%. In the SMPS operation mode, the number of particles exiting DMA1 was counted by a condensation particle counter (CPC, Model 3771, TSI Inc.) as the DMA1 voltage was continuously scanned. To determine hygroscopicity, particles of a known size selected in DMA1 were sent to an elevated RH environment in the Nafion™ humidifier (PD-070-18T-24SS, Perma Pure Inc.). Subsequently, the humidified aerosol passed through DMA2 where the voltage was exponentially ramped up and then backed down as described by Gasparini et al. (2006). The resulting hygroscopically resolved aerosol was counted by the CPC. The software for system operation and data inversion

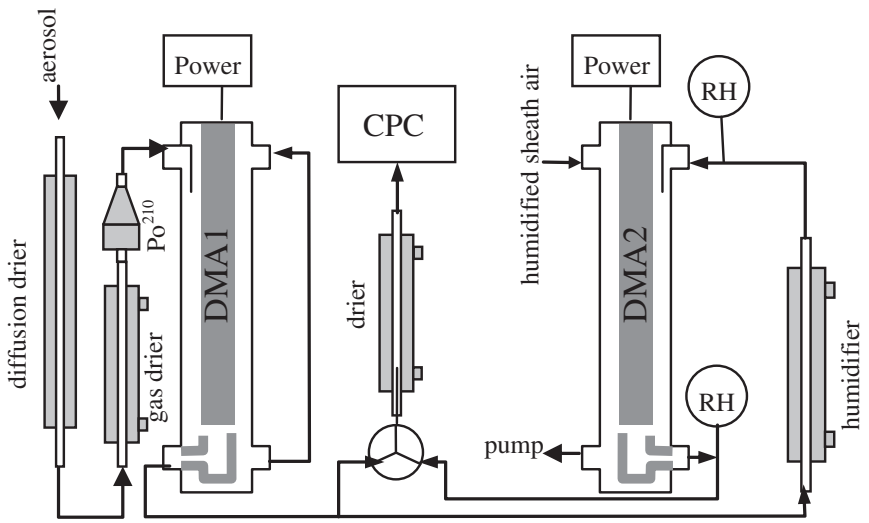

Fig. 1. Schematic diagram of the Hygroscopic Tandem Differential Mobility Analyzer (HTDMA) system.

was kindly donated by the Department of Atmospheric Sciences, Texas A&M University.

2.2. Hygroscopic growth factor and model calculation

The hygroscopic growth factor (GF) is defined herein as the relative increase in mobility diameter of dry particles due to water uptake at a certain RH, as expressed below:

$$GF(RH) = \frac{D_p}{D_{p,0}} \quad (1)$$

Where D_p is the mean mobility diameter for each hygroscopic mode at a specific RH and $D_{p,0}$ is the initial dry particle mobility diameter selected.

On assumption of particles consisting of a completely hydrophobic core coated by hygroscopic substances, hygroscopicity model has been widely applied to estimate the hygroscopic volume fraction of each hygroscopic particle group (Massling et al., 2009; Swietlicki et al., 1999). In our work, the chemical characteristic for the more-hygroscopic mode was partitioned as an internal mixture of hygroscopic inorganic component and inactive substances. Ammonium sulfate (AS) was chosen as reference in the model. The hygroscopic volume fraction (ε) was calculated by

$$\varepsilon = \frac{GF_2^3 - GF_1^3}{GF(AS)^3 - GF_1^3} \quad (2)$$

Where GF(AS) is the theoretical growth factor of ammonium sulfate, and GF_1 and GF_2 are retrieved growth factors of less and more hygroscopic mode, respectively.

2.3. Measurement site

The sampling site was located at the roof of the building of the Department of Environmental Science and Engineering at Fudan University (31°18'N, 121°29'E). The campus of Fudan University is located at a sub-center of the city, adjacent to Baoshan industrial zone in the northwest. With the contribution of mixed pollutant sources such as traffic, residential, and industrial emissions, the sampling site can be considered to be a representative of urban area. Ambient aerosols were transferred to the online instruments placed in the air-conditioned laboratory through a 4 m long copper tube with a diameter of 0.5 in. The inlet of the sampling tube was about 5 m above the ground and 0.5 m above the roof of the building.

2.4. Measurement methods

Measurements of particle size distribution and hygroscopic growth were conducted at 21 °C using the HTDMA system. The sampling was conducted in the late morning and afternoon during the period between January 30 and February 11 and in the day of February 18 in 2009, in metrological view of winter. However, the water-bubbling tank of HTDMA did not work properly on February 4. The data measured on Feb 10 was not discussed here when the HTDMA was connected to an Aerosol Time-of-Flight Mass Spectrometer (ATOFMS, TSI3800). The performance test of PSL spheres and ammonium sulfate prior to the observation showed no distinct difference from results reported by Ye et al. (2009), confirming that the HTDMA worked properly. The particle size distribution of submicrometer ambient aerosols with diameters of 20–400 nm was measured about once an hour. The measurement range was divided into 60 bins and scanned in 90 s; the total duration needed to measure particle size distribution was about 5 min. To determine the size-resolved hygroscopicity, dry particles with diameters of 30, 50, 100, 150, 200, and 250 nm were selected and humidified at 85% RH. TDMA tests were also carried out at RH = 20% to obtain the growth correction factor for each dry diameter. To investigate the deliquescence behavior, the hygroscopic growth factor against RH was measured on February 18. The local meteorological data including temperature, relative humidity, wind speed and direction, and atmospheric visibility were provided by the Shanghai Meteorological Bureau. The mixed layer height analysis was performed using the Real-time Environmental Applications and Display System (www.arl.noaa.gov).

3. Results and discussion

3.1. Metrological conditions

There was no precipitation during the field measurement campaign. Fig. 2 displays the hourly variations of temperature, relative humidity, wind direction and speed, as well as atmospheric visibility and mixed layer height between January 30 and February 11. The prevailing winds during this period were mainly from northeast to slightly northwest, and consequently air parcels arriving in Shanghai's urban area were influenced by pollutant emissions from suburb industrial areas and Jiangsu Province. An exception is that on February 1, clean and moist air parcels from the East China Sea passed through the city because the prevailing wind was easterly. The average visibility during the whole period was about 5 km with an hourly maximum of 15.6 km and an hourly minimum of 0.4 km, and about 80% of the days were under haze pollution. The largest daily average visibility of 9.6 km appeared on January 30, perhaps due to the scavenging effect of precipitation just before our observation. However, the hourly visibility decreased so rapidly that it dropped to 1 km in less than 40 hours. Another clear day was February 1, perhaps due to the contribution of eastern advection. The mixed layer height displayed a diurnal fluctuation similar to visibility. The average mixed layer height was about 400 m with a maximum of 1230 m and a minimum of 66 m, and this may have a significant impact on the pollutant dispersion.

3.2. Hygroscopic growth factor and particle mixing state

The hygroscopic growth factor distributions were mostly measured at a fixed relative humidity of 85%, ensuring that all hygroscopic particles were initially hydrated before entering DMA2. Similar to the results reported by Chen et al. (2003) and Santarpia et al. (2004), two distinct modes were present in all of the measured hygroscopic growth factor distributions except for the 30 nm particles during some periods. Fig. 3 shows a case of the hygroscopic growth factor distribution for particles in dry diameters of 30–200 nm at 85% RH. This case was measured on Februray 6. The hygroscopic growth factor distributions for 50–200 nm particles split into two groups,

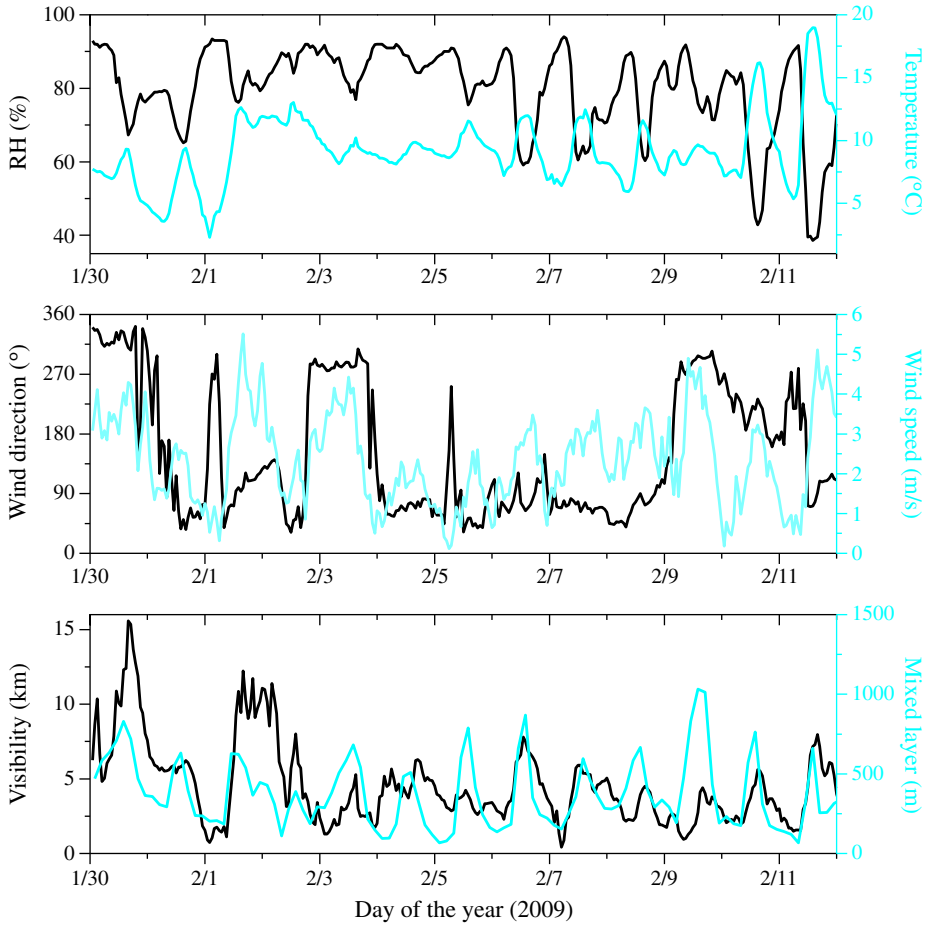

Fig. 2. Temperature, relative humidity, dewpoint, wind direction and speed, visibility and mixed layer height from January 30 to February 11 measured near Fudan University.

and the intensity of the second peak increased with the particle size. The appearance of bimodal distribution revealed that there may be more uptake of water on some particles, implying that the atmospheric aerosol was an external mixture of less and more hygroscopic particles. The strong peak tail in the hygroscopic growth factor distribution of 30 nm particles was indicative of hygroscopic particles.

Gaussian and lognormal models were frequently applied in the literature to parameterize the hygroscopic growth factor distribution and obtain the growth factor and number fraction of each hygroscopic particle group. In this study, the hygroscopic growth factor distributions were parameterized by fitting with one or more Gaussians since the retrieval back through peakfitted curves were in good agreement with the measured scatterplots. After parameterization by fitting with a sum of Gaussian distributions, most of the hygroscopic growth factor distributions were partitioned into two groups: less-hygroscopic mode (GF<1.15) and more-hygroscopic mode (GF>1.20). The less-hygroscopic group exhibited GFs in the range of 1.01–1.14, typically lower than 1.10. Fig. 4 displays the GF box of the less-hygroscopic group at each dry diameter. The median GFs of the less-hygroscopic particle group decreased steadily with the increase of particle size in the order of 1.08, 1.07, 1.06, 1.05, and 1.05 for 30, 50, 100, 150, and 200 nm particles, respectively. A similar finding was reported by Swietlicki et al. (1999). These nearly nonhygroscopic particles were assumed to consist mainly of black carbon and less- or non-hygroscopic organic species (Massling et al., 2009).

The number fraction is defined as the ratio of the particle number in one hygroscopic group to the total particle number of the hygroscopic growth factor distribution. Fig. 5 illustrates the number fraction of the less-hygroscopic mode at each dry diameter. The number fraction of the less-hygroscopic mode fluctuated intensively, possibly due to the variation of primary emission and secondary aerosol formation. The sulfate formation for newly nucleated particles was supposed to be important in some cases because the less-hygroscopic number fraction was observed to be as low as 0.1 for 30 nm particles. The average number fractions during the whole observation were 0.33, 0.25, 0.19, 0.18, and 0.17 for 30, 50, 100, 150, and 200 nm particles, respectively, indicating that the number fraction of less-hygroscopic group for Aitken mode particles ($D_{p,0}$<100 nm) should exceed that of accumulation mode particles ($D_{p,0}\geq$100 nm), consistent with those findings reported previously (Massling et al. 2009; Swietlicki et al., 1999). The fact that the number fraction of less hygroscopic particles decreased with increasing dry particle size could be due to several reasons: 1. Fresh soot from traffic source is predominantly emitted in Aitken mode; 2. Sulfate source from Jiangsu Province provided by long-

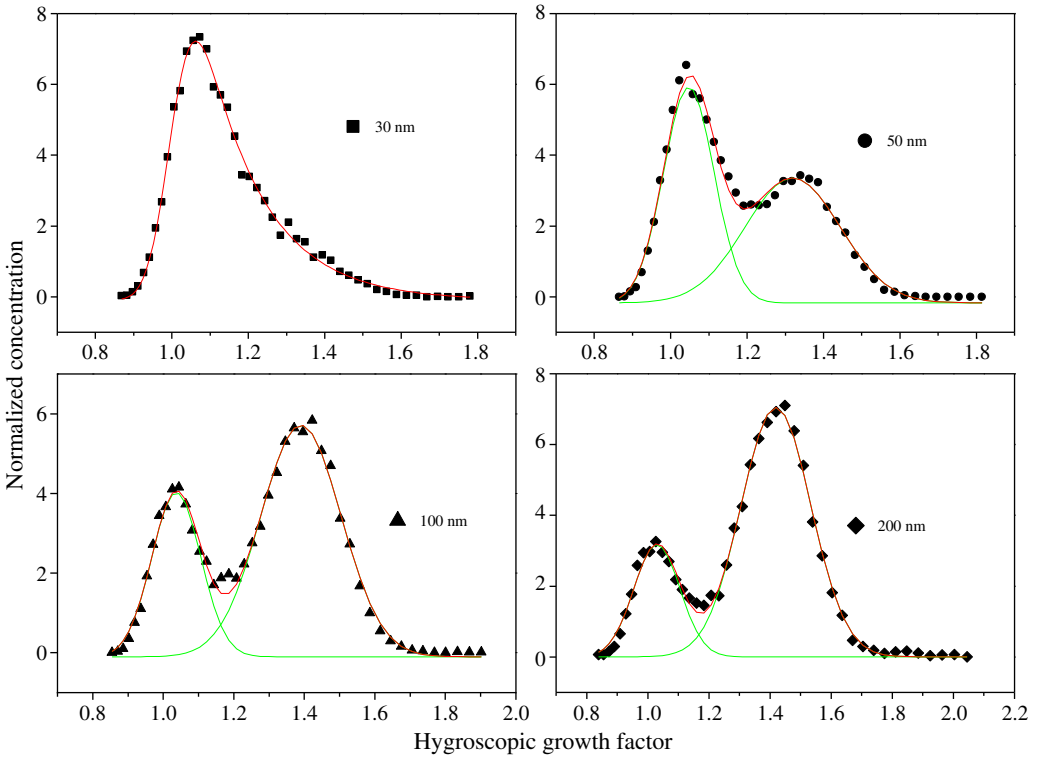

Fig. 3. An example of hygroscopic growth factor distribution for 30, 50, 100, and 200 nm particles exposed at 85% RH. The scatterplots denote the measured data while the green curve is Gaussian fit peak.

range transport only contributes to accumulation mode aerosols. 3. Atmospheric processing of Aitken mode particles is expected to result in a substantial increase in hygroscopic growth because of heavily sulfate pollution in Shanghai during wintertime. The number fractions of the less hygroscopic particles in this study were somewhat lower than those found in Leipzig and Beijing (Massling et al., 2005, 2009). It was reported that domestic heating through fossil fuel and coal burning contributed greatly to the urban ambient aerosols in those two cities during wintertime. However, these domestic heating techniques are not available in Shanghai. The average less-hygroscopic fraction was below 50% even for 30 nm particles, implying that a large

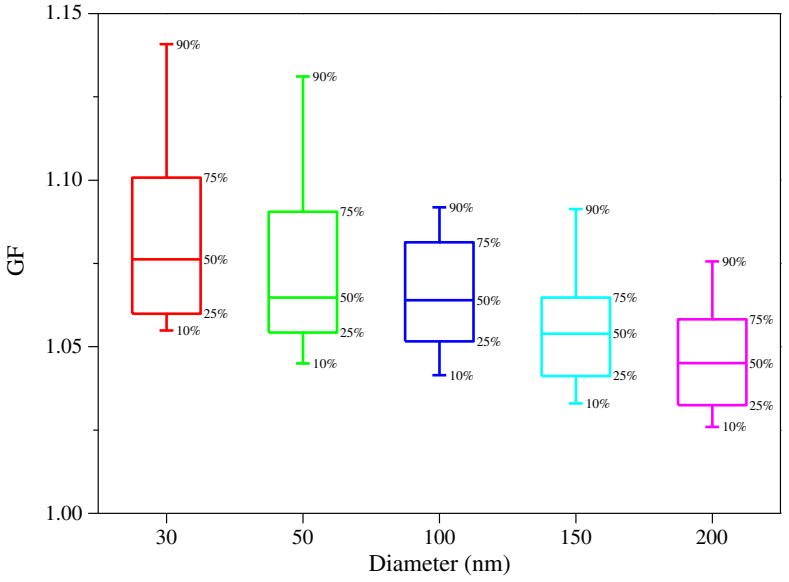

Fig. 4. Hygroscopic growth factor probability density of the less-hygroscopic group at each dry diameter over the whole campaign. The horizontal bar in each box represents the median, the box spans the range from the 25th to the 75th percentiles, and the whiskers denote the 10th and 90th percentiles.

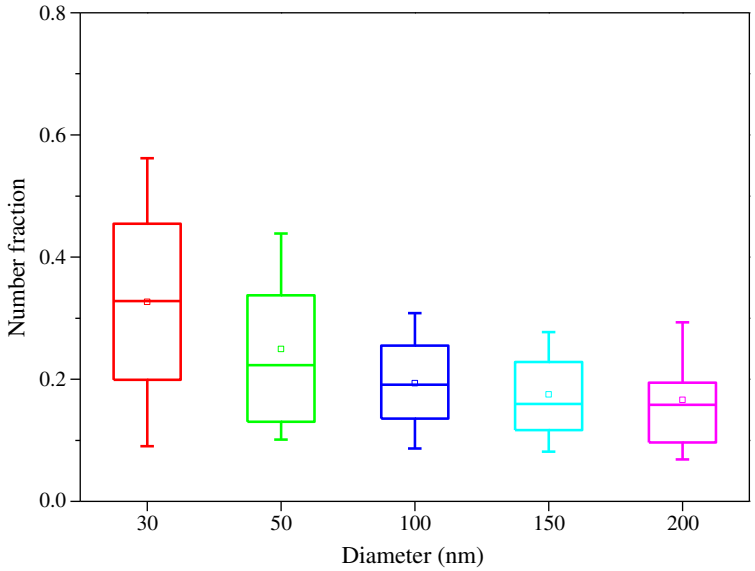

Fig. 5. Box plots showing the number fraction of the less-hygroscopic group at each dry diameter over the whole campaign. The horizontal bar in each box represents the median, the box spans the range from the 25th to the 75th percentiles, and the whiskers denote the 10th and 90th percentiles.

fraction of nucleated materials were hygroscopic. Because the hygroscopic behavior of the accumulation mode particles could not be explained by the coagulation of Aitken mode particles, we suppose that it was the condensation of some hygroscopic compounds rather than the coagulation that caused the growth of newly formed particles. In Shanghai, secondary inorganic aerosol should be the most important source of ambient aerosol hygroscopicity, as supported by the pollutant inventory. First, SO_2 and NO_x emissions in Shanghai were 2–3 times as those in Beijing (Chan and Yao, 2008); Secondly, SO_4^{2-}, NO_3^-, and NH_4^+ were the dominant ionic species, accounting for 46%, 18%, and 17% of the total mass of ions in PM2.5 (Yao et al., 2002); Thirdly, the monthly average low-cloud coverage varied from 30% to 40% (Xu et al., 1997), suggesting that aqueous-phase reactions may play an important role in the formation of secondary inorganic aerosols.

Fig. 6 illustrates the hygroscopic growth factor variation of the more-hygroscopic particles at each dry diameter. The median GFs showed a significant difference between Aitken and accumulation mode particles, nearly 1.3 in the size range of Aitken mode whereas it was above 1.4 for accumulation mode particles. This trend was also observed by Gasparini et al. (2006) who reported that the GF of more-hygroscopic mode increased with the particle size in the diameter range below 350 nm. The large gap in the hygroscopic growth factor between Aitken and accumulation mode particles observed in

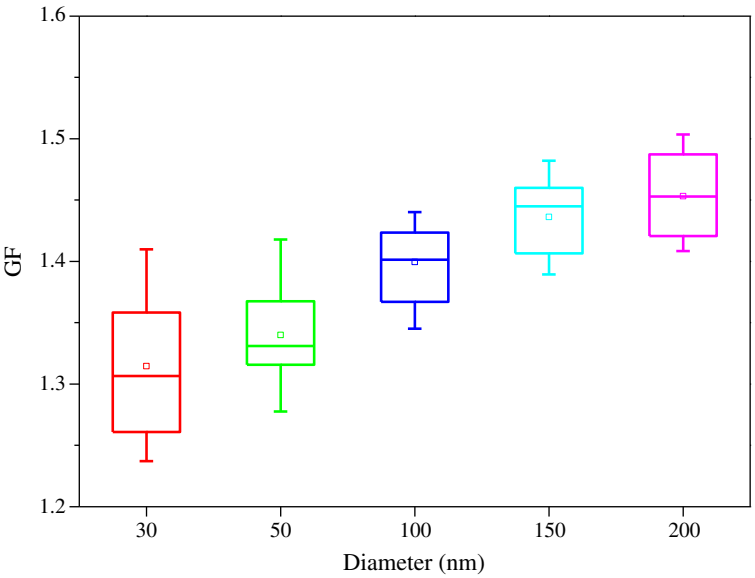

Fig. 6. Hygroscopic growth factor probability density of the more-hygroscopic group at each dry diameter over the whole campaign. The horizontal bar in each box represents the median, the box spans the range from the 25th to the 75th percentiles, and the whiskers denote the 10th and 90th percentiles.

this study indicates their difference in chemical composition, because it is beyond the Kelvin effect. In comparison with the GFs of pure ammonium sulfate and nitrate, the measured GFs are smaller than those of inorganic salts even for 200 nm particles. These phenomena suggest that the more-hygroscopic particles consisted mainly of insoluble materials and inorganic salts with internal mixing. The hygroscopic growth factors reported here are higher than those at the Southern Great Plains site (Gasparini et al., 2006), implying the higher contribution of inorganic pollutant emission.

The more-hygroscopic group has drawn much attention because it contributed a large number fraction. Swietlicki et al. (1999) postulated that the hygroscopic growth could be attributed entirely to the inorganic content of aerosol: sulfate, nitrate, and ammonium ions. However, many researchers suggested that water-soluble organics may affect the hygroscopic behavior of aerosols. In this study, the inorganic fraction of the less-hygroscopic mode is ignored and the insignificant hygroscopic growth at 85% RH is assumed to be due to the contribution of organics in aerosols. The GF of the less-hygroscopic mode is used to partition the more hygroscopic particles into hygroscopically active and inactive fractions to estimate the content of hygroscopic inorganic substances. Ammonium sulfate has been widely recommended as a model compound to calculate the hygroscopic volume fraction of individual particles on the basis of these features: 1. Neutralized sulfate and nitrate aerosols constitute a large mass fraction of the submicrometer aerosol in back-ground continental air masses (Heintzenberg, 1989); 2. Particles consisting of both sub- and super-saturated solutions of ammonium sulfate and ammonium nitrate show quite similar hygroscopic growth (Chan et al., 1992); 3. Small amounts of NaCl, KCl, and their internal mixtures in atmospheric nanoparticles do not contribute to the obvious hygroscopic growth (Chen et al., 2003). The chemical measurements on atmospheric aerosols in Shanghai were reported previously, and the major ion concentrations of PM2.5 are summarized in Table 1. Sulfate was the most abundant ion species during wintertime, and its average concentration was 12.79–22.29 μg m^{-3}. The sum of sulfate, nitrate, and ammonium was about 25–37 μg m^{-3}, about 6 times higher than the total amount of Na^+, K^+, and Cl^-. For this reason, ammonium sulfate was chosen as the reference in our model calculation. The theoretical growth factor of ammonium sulfate was calculated using a hygroscopic growth factor calculator downloaded from http://collinsgroup.tamu.edu/labview.php.

Fig. 7 illustrates the hygroscopic volume fractions of more hygroscopic particles. Averaged over the whole period, the hygroscopic volume fraction was about 0.47, 0.50, 0.61, 0.70, and 0.70 for the more hygroscopic population of 30, 50, 100, 150, and 200 nm particles, respectively, indicating that 30 nm particles should be composed of 47% hygroscopic inorganic substances, whereas the estimated value is 70% for 200 nm particles. The difference in the hygroscopic volume fraction between Aitken and accumulation mode particles supports our assumption that the particle growth is mainly attributed to the condensation of sulfate and nitrate. Massling et al. (2009) reported that the average GFs in Beijing were 1.26, 1.40, and 1.51 for 30, 50, and 150 nm particles, corresponding to 0.34, 0.51, and 0.67 of modeled soluble volume fraction. Our findings are consistent with these data except that a larger GF for 30 nm particles was observed in our work. The possible explanation for the exception is the higher emission of carbonaceous material at the Beijing site due to the high emission of traffic-related aerosols in combination with domestic heating with fossil fuels and the use of coal-fired heating plants (Massling et al., 2009).

To obtain information about the temporal variation of chemical composition based on the hygroscopic behavior, we focused on the number fraction of more hygroscopic particles with a diameter of 100 nm and the corresponding modeled hygroscopic volume fraction of individual particles between 12:00 and 18:00 during the first week in February, when both temperature and RH were very stable while clear changes in wind direction and speed took place. As illustrated in Fig. 8, the hygroscopic volume fraction decreased sharply on February 2. We assume that the decrease was due to the change in mixed layer height and advection of air masses. Generally, the hygroscopic volume fraction decreased with time in each afternoon except February 2. The most plausible explanation for the hygroscopic contribution cycles is the condensation of sulfate and secondary organic aerosol. The production of sulfate both through gas phase and aqueous phase reactions is expected to peak in the late morning and early afternoon during wintertime when the concentrations of $OH^{\cdot}$ and H_2O_2 are the highest. On the other hand, the adsorption of soot and organic aerosol on the particle surface would decrease its water uptake. Another expected variation is that the daily average hygroscopic fraction increases with time. However, this was not observed in our measurements.

3.3. Dependence of hygroscopic growth on relative humidity

Ambient aerosol is mainly composed of sulfates, nitrates, ammonium, sea salt, hydrogen ions, crust components, and organic materials with different hygroscopic behaviors. Whether the aerosol components are internally or externally mixed, they are vital to atmospheric visibility. For NH_4NO_3–$(NH_4)_2SO_4$ system, the aerosols as external mixture showed larger visibility reduction than their counterparts as internal mixtures (Tang et al., 1981). Compared to the single component aerosol, the hygroscopic growth of an internally mixed-salt aerosol is complicated by the fact that a solid salt

Table 1
Concentrations of major ions of $PM_{2.5}$ in Shanghai (μg m^{-3}).

Year	Season	SO_4^{2-}	NO_3^-	NH_4^+	Cl^-	Na^+	K^+	R*	Reference
1999–2000	Winter	17.78	9.64	7.38	3.54	0.44	2.61	0.791	Ye et al., 2003
1997–2001	Winter	22.29	9.89	4.47	3.62	–	–	0.400	Xiu et al., 2004
1999–2000	Year	15.2	6.5	6.2	1.7	0.7	1.9	0.830	Yao et al., 2002
2003–2005	Winter	12.79	8.53	4.38	3.4	0.55	0.85	0.610	Wang et al., 2006

*$R = \frac{n_{NH_4^+}}{2n_{SO_4^{2-}} + n_{NO_3^-}}$, where $n_{NH_4^+}$, $n_{SO_4^{2-}}$ and $n_{NO_3^-}$ denote the molar concentration of NH_4^+, SO_4^{2-} and NO_3^-, respectively.

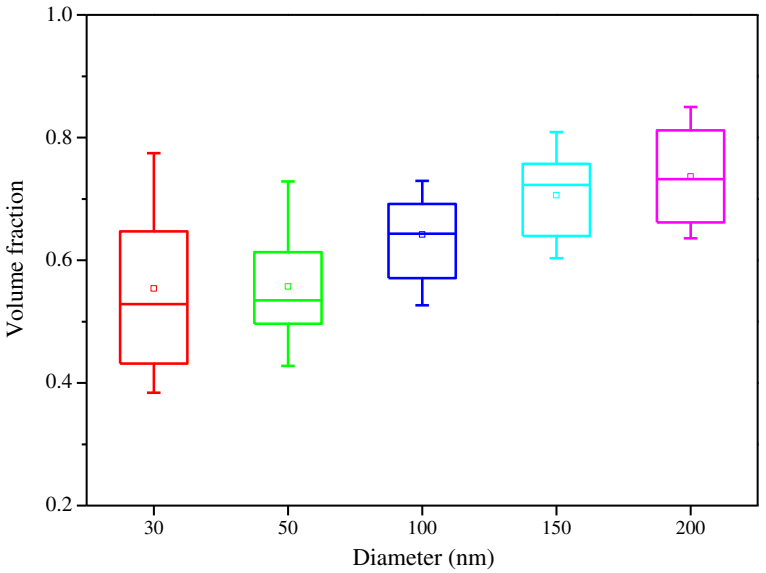

Fig. 7. Box plots showing to the volume fraction of modeled hygroscopic inorganic component in the individual particles of the more-hygroscopic group at each dry diameter over the whole campaign. The horizontal bar in each box represents the median, the box spans the range from the 25th to the 75th percentiles, and the whiskers denote the 10th and 90th percentiles.

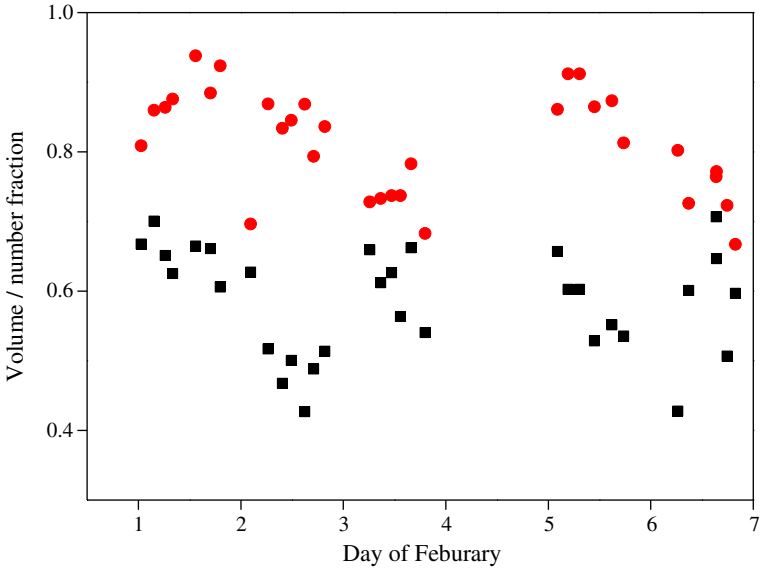

Fig. 8. Temporal variation of the number fraction of more hygroscopic particles with a diameter of 100 nm dry diameter and corresponding modeled hygroscopic volume fraction of individual particles between 12:00 and 18:00 during the first week in February. (●) number fraction of more hygroscopic particles; (■) modeled hygroscopic volume fraction of individual particles.

particle may go through several regions of multiphase equilibrium before it is completely dissolved to form a homogeneous solution droplet. The first deliquescence point of the NH_4NO_3–$(NH_4)_2SO_4$ system with molar sulfate to nitrate ratio of 3 occurs at RH = 65.7%, whereas the second-stage growth occurs at RH = 76.8% when the system has become a saturated solution droplet (Wexler and Seinfeld, 1991). Investigation of hygroscopicity against RH can provide insight into the chemical composition and the mixing state of an aerosol. Fig. 9a displays the hygroscopic growth factor distributions of atmospheric particles after humidification at RHs in one case. This case was measured on February 18. For 30 nm particles, no obvious change in the hygroscopic growth factor distribution was observed between 20% and 70% RH,

Fig. 9. (a) Hygroscopic growth factor distribution against RH at each dry diameter. The particle sizes are labeled in the chart. (b) Hygroscopic growth factor and deliquesced fraction as a function of RH. The particle sizes are labeled in the chart.

a

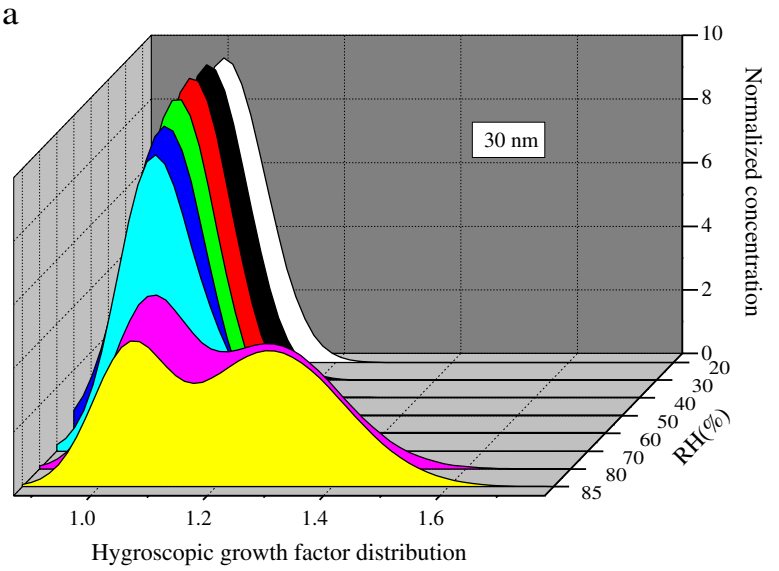
30 nm
Normalized concentration
0
2
4
6
8
10
20
30
40
50
60
70
80
85
RH(%)
1.0
1.2
1.4
1.6
Hygroscopic growth factor distribution

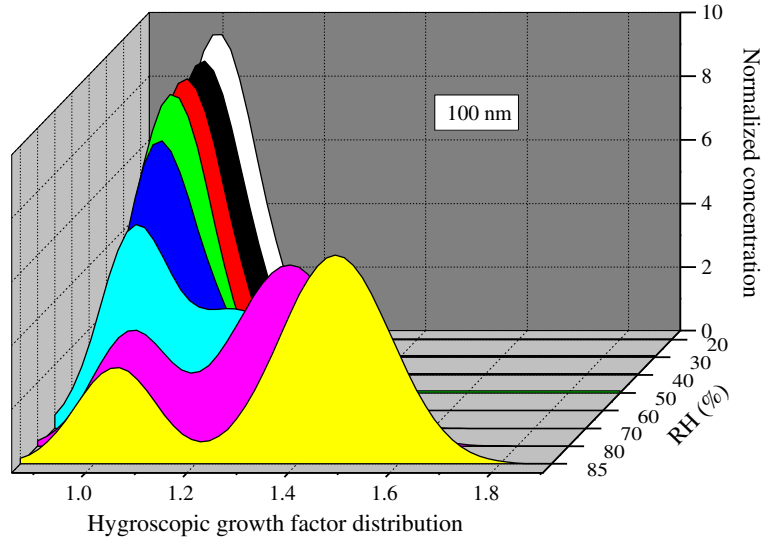
100 nm
Normalized concentration
0
2
4
6
8
10
20
30
40
50
60
70
80
85
RH (%)
1.0
1.2
1.4
1.6
1.8
Hygroscopic growth factor distribution

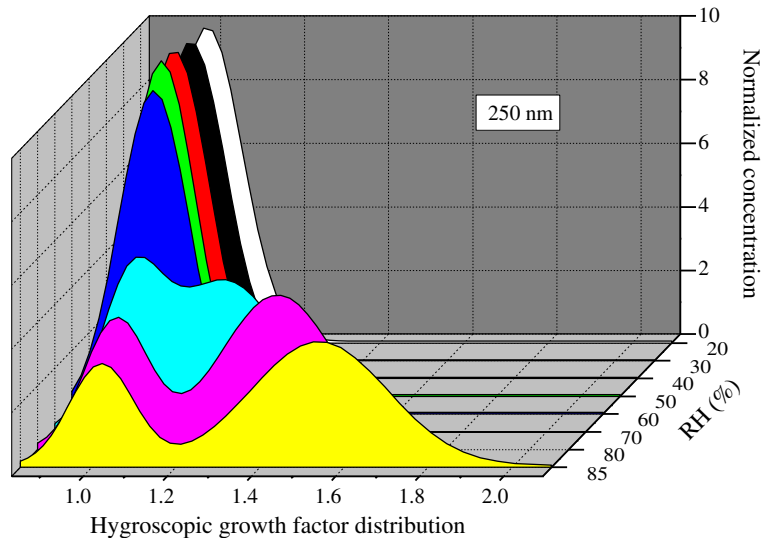
250 nm
Normalized concentration
0
2
4
6
8
10
20
30
40
50
60
70
80
85
RH (%)
1.0
1.2
1.4
1.6
1.8
2.0
Hygroscopic growth factor distribution

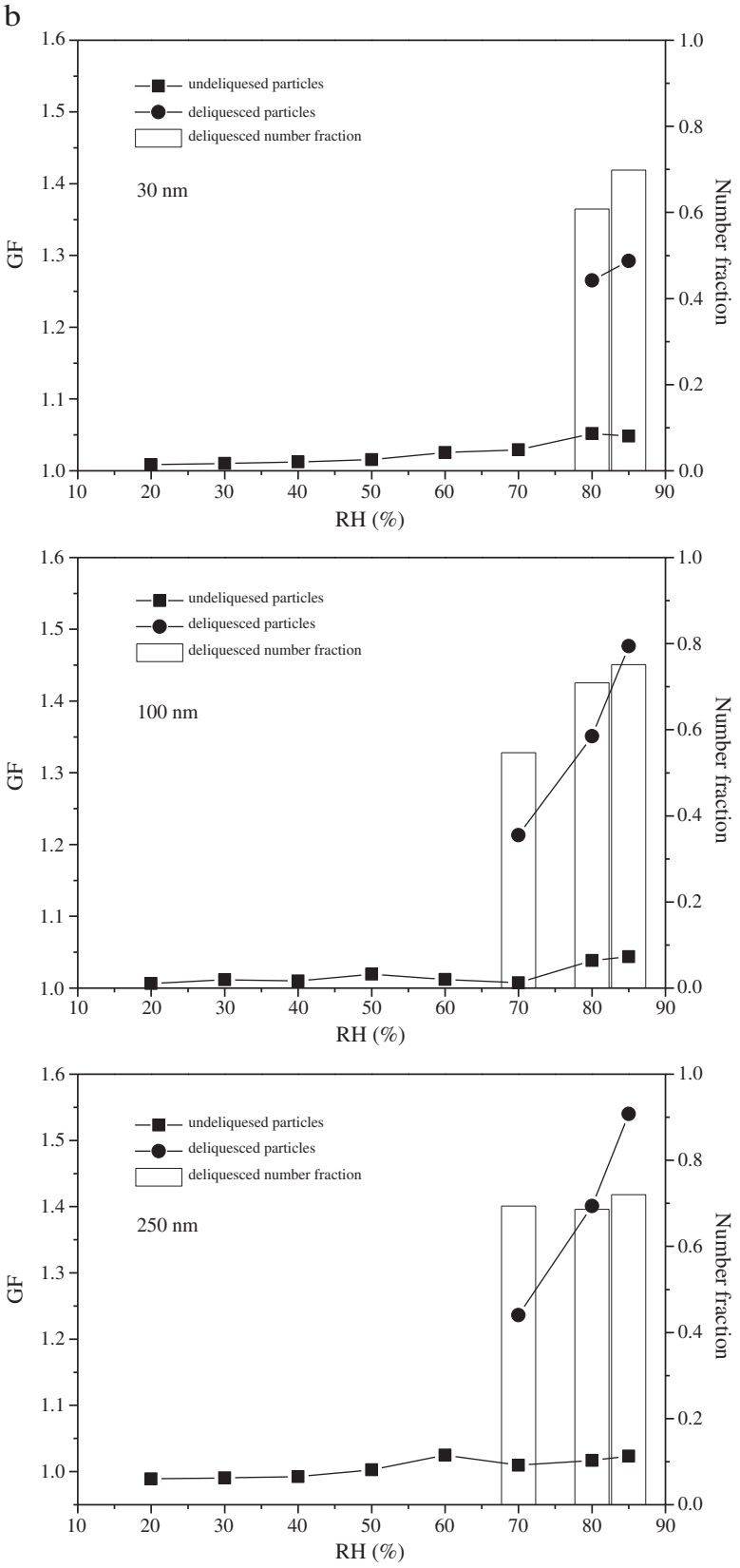

Fig. 9 (*continued*).

indicating that no deliquescence took place. The splitting growth phenomenon abruptly appeared at 80% RH, suggesting that the 30 nm particle population consisted of at least two hygroscopic groups in the external mixing state. Different from 30 nm particles, the splitting growth phenomena for 100 and 250 nm particles were observed at RH = 70%. The second peak shifted to a larger GF value with the further increase of RH, whereas the intensity of the first peak decreased.

To obtain detailed information on the mixing state of the aerosol, GF value and deliquesced fraction were quantified. Fig. 9b shows the variations of the hygroscopic growth factor and the number fraction of deliquesced particles against RH. For all measurements, the growth factor was below 1.05 when RH<60%. The small shrinking was attributed to system experimental error. It is concluded that the aerosols contain a negligible amount of ammonium bisulfate with the deliquescence RH at 39%, supporting our assumption that the contribution of hygroscopic growth should be attributed to ammonium nitrate and ammonium sulfate. The absence of ammonium bisulfate was also supported by the chemical analysis of Wang et al. (2006). They reported that ammonium bisulfate only contributed 0.1 ng cm^{-3} to PM2.5 in Shanghai during wintertime. The absence of hygroscopic growth at 70% RH suggested that ammonium nitrate had a minor contribution to the population of 30 nm particles. The hygroscopic growth above 80% RH should be attributed to ammonium sulfate, in agreement with the theoretical deliquescence behavior of ammonium sulfate. These conclusions are supported by similar results reported previously. During the Asian outflow episodes in January 2003, Chou et al. (2005) found that sulfate in atmospheric particles in Taipei with a cut diameter of 0.1 μm was significant whereas nitrate was negligible. The deliquesced fraction at 70% RH was 55% for the population of 100 nm particle, indicating the existence of internal mixture of ammonium nitrate and ammonium sulfate with a significant amount of ammonium nitrate. Compared to 100 nm particles, 250 nm particles displayed a larger deliquesced number fraction at 70% RH, implying a larger contribution of ammonium nitrate. These findings suggested that the mass fraction of ammonium nitrate in hygroscopic particles increased with the particle size. Based on 1.61 of the theoretical GF of ammonium nitrate at 85% RH, we could imagine that hygroscopic particles with $D_{p,0} = 250$ nm were internal mixtures containing some hygroscopically inactive materials. The enhanced nitrate content of larger particles is possibly a result of heterogeneous reaction of nitrate precursors with sulfate-containing particles, and this is further favored by the occurrence of deliquescence. Considering the high RH during the whole campaign, we can postulate that most of the accumulation mode particles were deliquesced. The effect of deliquescence on the oxidation process of SO_2 and NO_x as well as scattering albedo under haze condition should be investigated further.

4. Conclusions

The size-resolved hygroscopicity of submicrometer aerosol particles in Shanghai's urban area was measured using a HTDMA during a highly polluted period between January 30 and February 11 and in the day of Feb 18 in 2009. Bimodal size distribution was almost always observed after exposure to 85% RH for the selected monodisperse aerosol at each dry diameter. The hygroscopic growth factors varied with particle size. The less-hygroscopic group was nearly hydrophobic. The number fraction of the less-hygroscopic group for Aitken mode particles was larger than that of the accumulation mode. The fact that the less-hygroscopic fraction was somewhat lower than those found in Leipzig and Beijing was assumed to be due to the difference in domestic heating technique. The modeled hygroscopic volume fraction suggested that accumulation mode particles were dominated by secondary inorganic aerosols whereas Aitken mode particles consisted of a relatively larger amount of insoluble carbonaceous materials. The deliquescence against RH curves showed that ammonium bisulfate made no contribution to submicrometer aerosols in Shanghai's urban area. The enhanced nitrate content of accumulation mode particles in comparison with the absence of nitrate in Aitken mode particles revealed that the addition of nitrate was initially promoted by sulfate condensation during atmospheric particle aging process.

Acknowledgments

The authors are thankful for the financial support from the National Natural Science Foundation of China (Grant Nos. 40775080, 40875073, 41075088, and 20937001) and the Research Fund for the Doctoral Program from Ministry of Education (Grant No. 20070246024).

References

Achtert, P., Birmili, W., Nowak, A., Wehner, B., Wiedensohler, A., Takegawa, N., Kondo, Y., Miyazaki, Y., Hu, M., Zhu, T., 2009. Hygroscopic growth of tropospheric particle number size distributions over the North China Plain. Journal of Geophysical Research-Atmospheres 114, D00G07.

Aggarwal, S.G., Mochida, M., Kitamori, Y., Kawamura, K., 2007. Chemical closure study on hygroscopic properties of urban aerosol particles in Sapporo, Japan. Environmental Science and Technology 41, 6920–6925.

Baltensperger, U., Streit, N., Weingartner, E., Nyeki, S., Prevot, A.S.H., Van Dingenen, R., Virkkula, A., Putaud, J.P., Even, A., ten Brink, H., Blatter, A., Neftel, A., Gaggeler, H.W., 2002. Urban and rural aerosol characterization of summer smog events during the PIPAPO field campaign in Milan, Italy. Journal of Geophysical Research -Atmospheres 107 (D22), 8193.

Boucher, O., Anderson, T.L., 1995. General circulation model assessment of the sensitivity of direct climate forcing by anthropogenic sulfate aerosols to aerosol size and chemistry. Journal of Geophysical Research-Atmospheres 100 (D12), 26117–26134.

Chan, C.K., Yao, X., 2008. Air pollution in mega cities in China. Atmospheric Environment 42, 1–42.

Chan, C.K., Flagan, R.C., Seinfeld, J.H., 1992. Water activities of NH_4NO_3/$(NH_4)_2SO_4$ solutions. Atmospheric Environmental 26, 1661–1673.

Chan, H.K., Eberl, S., Daviskas, E., Constable, C., Young, I., 2002. Changes in lung deposition of aerosols due to hygroscopic growth: a fast SPECT study. Journal of Aerosol Medicine-Deposition Clearance and Effects in the Lung 15, 307–311.

Chen, L.Y., Jeng, F.T., Chen, C.C., Hsiao, T.C., 2003. Hygroscopic behavior of atmospheric aerosol in Taipei. Atmospheric Environment 37 (15), 2069–2075.

Chou, C.C., Huang, S., Chen, T., Lin, C., Wang, L., 2005. Size-segregated characterization of atmospheric aerosols in Taipei during Asian outflow episodes. Atmospheric Research 75, 89–109.

Cocker, D.R., Whitlock, N.E., Flagan, R.C., Seinfeld, J.H., 2001. Hygroscopic properties of Pasadena, California aerosol. Aerosol Science and Technology 35, 637–647.

Davis, E.J., Buehler, M.F., Ward, T.L., 1990. The double-ring electrodynamic balance for microparticle characterization. Review of Scientific Instruments 61, 1281–1288.

Day, D.E., Hand, J.L., Carrico, C.M., Engling, G., Malm, W.C., 2006. Humidification factors from laboratory studies of fresh smoke from biomass fuels. Journal of Geophysical Research-Atmospheres 111 (D22), D22202.

Dentener, F.J., Crutzen, P.J., 1993. Reaction of N_2O_5 on tropospheric aerosols: impact on the global distributions of NO_x, O_3, and OH. Journal of Geophysical Research - Atmospheres 98, 7149–7163.

Eichler, H., Cheng, Y.F., Birmili, W., Nowak, A., Wiedensohler, A., Brueggemann, E., Gnauk, T., Herrmann, H., Althausen, D., Ansmann, A., Engelmann, R., Tesche, M., Wendisch, M., Zhang, Y.H., Hu, M., Liu, S., Zeng, L.M., 2008. Hygroscopic properties and extinction of aerosol

particles at ambient relative humidity in South-Eastern China. Atmospheric Environment 42, 6321–6334.
Ferron, G.A., Karg, E., Busch, B., Heyder, J., 2005. Ambient particles at an urban, semi-urban and rural site in Central Europe: hygroscopic properties. Atmospheric Environment 39, 343–352.
Fu, Q., Zhuang, G., Wang, J., Xu, C., Huang, K., Li, J., Hou, B., Lu, T., Streets, D.G., 2008. Mechanism of formation of the heaviest pollution episode ever recorded in the Yangtze River Delta, China. Atmospheric Environment 42, 2023–2036.
Gasparini, R., Li, R., Collins, D.R., Ferrare, R.A., 2006. Application of aerosol hygroscopicity measured at the Atmospheric Radiation Measurement Program's Southern Great Plains site to examine composition and evolution. Journal of Geophysical Research – Atmospheres 111, D05S12.
Gasso, S., Hegg, D.A., Covert, D.S., 2000. Influence of humidity on the aerosol scattering coefficient and its effect on the upwelling radiance during ACE-2. Tellus Series B-Chemical and Physical Meteorology 52, 546–567.
Geng, F., Tie, X., Xu, J., Zhou, G., Li, P., Gao, W., Tang, X., Zhao, C., 2008. Characterizations of ozone, NO_x and VOCs measured in Shanghai, China. Atmospheric Environmental 42, 6873–6883.
Heintzenberg, J., 1989. Fine particles in the global troposphere, a review. Tellus Series B-Chemical and Physical Meteorology 41, 149–160.
Kotchenruther, R.A., Hobbs, P.V., Hegg, D.A., 1999. Humidification factors for atmospheric aerosols off the mid-Atlantic coast of the United States. Journal of Geophysical Research-Atmospheres 104 (D2), 2239–2251.
Liu, B.Y.H., Pui, D.Y.H., Whitby, K.T., Kittelson, D.B., Kousaka, Y., McKenzie, R.L., 1978. Aerosol mobility chromatograph – new detector for sulfuric-acid aerosols. Atmospheric Environment 12, 99–104.
Liu, Y., Cain, J.P., Wang, H., Laskin, A., 2007. Kinetic study of heterogeneous reaction of deliquesced NaCl particles with gaseous HNO_3 using particle-on-substrate stagnation flow reactor approach. Journal of Physical Chemistry A 111, 10026–10043.
Liu, Y., Gibson, E.R., Cain, J.P., Wang, H., Grassian, V.H., Laskin, A., 2008. Kinetics of heterogeneous reaction of $CaCO_3$ particles with gaseous HNO_3 over a wide range of humidity. Journal of Physical Chemistry A 112, 1561–1571.
Londahl, J., Massling, A., Pagels, J., Swietlicki, E., Vaclavik, E., Loft, S., 2007. Size-resolved respiratory-tract deposition of fine and ultrafine hydrophobic and hygroscopic aerosol particles during rest and exercise. Inhalation Toxicology 19, 109–116.
Massling, A., Stock, M., Wiedensohler, A., 2005. Diurnal, weekly, and seasonal variation of hygroscopic properties of submicrometer urban aerosol particles. Atmospheric Environment 39, 3911–3922.
Massling, A., Stock, M., Wehner, B., Wu, Z.J., Hu, M., Brüggemann, E., Gnauk, T., Herrmann, H., Wiedensohler, A., 2009. Size segregated water uptake of the urban submicrometer aerosol in Beijing. Atmospheric Environment 43, 1578–1589.
McMurry, P.H., Stolzenburg, M.D., 1989. On the sensitivity of particle-size to relative-humidity for Los-Angeles aerosols. Atmospheric Environment 23, 497–507.
Mogili, P., Kleiber, P., Young, M., Grassian, V.H., 2006. N_2O_5 hydrolysis on the components of mineral dust and sea salt aerosol: comparison study in an environmental aerosol reaction chamber. Atmospheric Environment 40, 7401–7408.
Peng, C.G., Chan, C.K., 2001. The water cycles of water-soluble organic salts of atmospheric importance. Atmospheric Environment 35, 1183–1192.
Petters, M.D., Kreidenweis, S.M., 2007. A single parameter representation of hygroscopic growth and cloud condensation nucleus activity. Atmospheric Chemistry and Physics 7, 1961–1971.
Randall, D.A., Wood, R.A., Bony, S., Colman, R., Fichefet, T., Fyfe, J.V.K., Pitman, A., Shukla, J., Srinivasan, J., Stouffer, R.J., Sumi, A., Taylor, K.E., 2007. Contribution of Working Group I to the Fourth Assessment Report of the Intergovernmental Panel on Climate Change – Climate Models and their Evaluation. Cambridge University Press, Cambridge.
Rood, M.J., Larson, T.V., Covert, D.S., 1985. Measurement of laboratory and ambient aerosols with temperature and humidity controlled nephelometry. Atmospheric Environment 19, 1181–1190.
Santarpia, J.L., Li, R., Collins, D.R., 2004. Direct measurement of the hydration state of ambient aerosol populations. Journal of Geophysical Research -Atmospheres 109 (D18), D18209.
Svenningsson, B., Rissler, J., Swietlicki, E., Mircea, M., Bilde, M., Facchini, M.C., Decesari, S., Fuzzi, S., Zhou, J., Monster, J., Rosenorn, T., 2006. Hygroscopic growth and critical supersaturations for mixed aerosol particles of inorganic and organic compounds of atmospheric relevance. Atmospheric Chemistry and Physics 6, 1937–1952.
Swietlicki, E., Zhou, J., Berg, O.H., Martinsson, B.G., Frank, G., Cederfelt, S.I., Duse, K.U., Berner, A., Birmili, W., Wiedensohler, A., Yuskiewicz, B., Bower, K.N., 1999. A closure study of sub-micrometer aerosol particle hygroscopic behaviour. Atmospheric Research 50, 205–240.
Swietlicki, E., Hansson, H.C., Hameri, K., Svenningsson, B., Massling, A., McFiggans, G., McMurry, P.H., Petaja, T., Tunved, P., Gysel, M., Topping, D., Weingartner, E., Baltensperger, U., Rissler, J., Wiedensohler, A., Kulmala, M., 2008. Hygroscopic properties of submicrometer atmospheric aerosol particles measured with H-TDMA instruments in various environments - a review. Tellus Series B-Chemical and Physical Meteorology 60, 432–469.
Tang, I.N., Wong, T.W., Munkelwitz, H.R., 1981. The relative importance of atmospheric sulfates and nitrates in visibility reduction. Atmospheric Environment 15, 2463–2471.
Tursic, J., Berner, A., Podkrajsek, B., Grgic, L., 2004. Influence of ammonia on sulfate formation under haze conditions. Atmospheric Environment 38, 2789–2795.
Wang, Y., Zhuang, G., Zhang, X., Zhang, X., Huang, K., Xu, C., Tang, A., Chen, J., An, Z., 2006. The ion chemistry, seasonal cycle, and sources of PM2.5 and TSP aerosol in Shanghai. Atmospheric Environment 40, 2935–2952.
Wexler, A.S., Seinfeld, J.H., 1991. Second-generation inorganic aerosol model. Atmospheric Environment 25A, 2731–2748.
Xiu, G., Zhang, D., Chen, J., Huang, X., Chen, Z., Guo, H., Pan, J., 2004. Characterization of major water-soluble inorganic ions in size-fractionated particulate matters in Shanghai campus ambient air. Atmospheric Environment 38, 227–236.
Xu, J., Zhu, Y., Li, J., 1997. Seasonal cycles of surface ozone and NO_x in Shanghai. Journal of Applied Meteorology 36, 1424–1429.
Yan, P., Pan, X., Tang, J., Zhou, X., Zhang, R., Zeng, L., 2009. Hygroscopic growth of aerosol scattering coefficient: a comparative analysis between urban and suburban sites at winter in Beijing. Particuology 7, 52–60.
Yao, X., Chan, C., Fang, M., Cadle, S., Chan, T., Mulawa, P., He, K., Ye, B., 2002. The water-soluble ionic composition of PM2.5 in Shanghai and Beijing, China. Atmospheric Environment 36, 4223–4234.
Ye, B., Ji, X., Yang, H., Yao, X., Chan, C.K., Cadle, S.H., Chan, T., Mulawa, P.A., 2003. Concentration and chemical composition of PM2.5 in Shanghai for a 1-year period. Atmospheric Environment 37, 499–510.
Ye, X., Chen, T., Hu, D., Yang, X., Chen, J., Zhang, R., Khakuziv, A.F., Wang, L., 2009. A multifunctional HTDMA system with a robust temperature control. Advances in Atmospheric Sciences 26, 1235–1240.
Zhang, R., Khalizov, A.F., Pagels, J., Zhang, D., Xue, H., McMurry, P.H., 2008. Variability in morphology, hygroscopicity, and optical properties of soot aerosols during atmospheric processing. Proceedings of the National Academy of Sciences of the United States of America 105, 10291–10296.